Comput Mech (2007) 39: 719–728
DOI 10.1007/s00466-006-0061-x

ORIGINAL PAPER

I.V. Singh · Masa Tanaka · M. Endo

Thermal analysis of CNT-based nano-composites by element free Galerkin method

Received: 14 October 2005 / Accepted: 23 February 2006 / Published online: 25 March 2006

Abstract This paper deals with the thermal analysis of carbon nanotube (CNT) based composites by meshless element free Galerkin method. Cylindrical representative volume element (cylindrical RVE) has been chosen to evaluate the thermal properties of nano-composites using multi-domain and simplified approaches. The values of temperature have been calculated at different points and plotted against RVE length and RVE radius. A sensitivity analysis of RVE as well as CNT dimensions has been carried out in detail. The present computations show that the equivalent thermal conductivity is a function of CNT length, CNT radius, RVE length and RVE radius. Based on present numerical simulations, an approximate formula is proposed to calculate the equivalent thermal conductivity of nano-composites. The results obtained by simplified approach have been found in good agreement with those obtained by multi-domain approach.

Keywords Carbon nanotube · Nano-composites Thermal conductivity · Multi-domain approach Simplified approach · Meshless · Element free Galerkin method

Notations

k_{m_1}	thermal conductivity of matrix (W/m K)
k_{m_2}	thermal conductivity of carbon nanotube (W/m K)
k_{e}	equivalent thermal conductivity of composite (W/m K)
L	length of cylindrical RVE (nm)
L_c	CNT length (nm)
m	number of terms in the basis
m_1	matrix material
m_2	carbon nanotube material
n	number of nodes in the domain of influence
n'	outward normal to the surface
q	heat flux (W/m^2)
r_o	outer radius of CNT (nm)
R_o	radius of cylindrical RVE (nm)
t	thickness of CNT (nm)
T_{C}	constant temperature at CNT surface (K)
$T^h(\mathbf{r})$	MLS approximation function for temperature
w	weight function used in MLS approximation
$\bar{w}$	weighting function used in weak form
α	penalty parameter
Γ_3	CNT surface
Γ	boundary of the domain
Ω_1	domain for matrix
Ω_2	domain for CNT
$\Phi_I(\mathbf{r})$	shape function

I.V. Singh (✉) · M. Tanaka · M. Endo
Faculty of Engineering,
Shinshu University,
Nagano 380-8553, Japan
E-mail: iv_singh@yahoo.com

1 Introduction

In last decade, carbon nanotubes (CNTs) have attracted many researchers towards the field of nanotechnology due to their excellent physical, mechanical, electrical and thermal properties. These remarkable properties make the CNTs as an ideal reinforcing material for the composites. Many researchers believe that CNTs may provide us an entirely new class of composite materials (see the comprehensive review articles [1–10]). The mechanical and electrical properties of CNTs and CNT based composites have been studied by many researchers through experimental work [11–25], quantum mechanics [26–32], Monte-Carlo simulation [33–35], molecular dynamics [36–40] and continuum methods [41–55].

Thermal conduction plays a fundamentally critical role in the performance and stability of nano/micro devices. Therefore, the study of the thermal behavior of nano-materials becomes increasingly important with the reduction of device size. Few experiments were conducted to measure the thermal conductivity of mats (fabricated using compressed ropes of CNTs) [56, 57], and the value of thermal conductivity was found in the range of 1,750 to 5,850 W/m K. By direct experiment, the thermal conductivity of individual multi-walled CNT was found to be 3,000 W/m K at room temperature [58]. A higher value of thermal conductivity, i.e. 6,600 W/m K was

reported by molecular dynamics (MD) simulations at room temperature [59–61]. Biercuk et al. [62] observed an increase in thermal conductivity of 70% at 40 K and 125% at 300 K by addition of 1% (by weight) single walled nanotubes. Heat conduction of finite-length single-walled carbon nanotubes (SWNTs) was carried out by Maruyama [63] using MD approach with Tersoff-Brenner bond order potential, and the thermal conductivity was calculated with Fourier's law from the measured temperature gradient and the energy budgets in phantom molecules. Thermal conductivity of carbon nanotubes and diamond nanowires with atomic interactions was modeled by Brenner potential using MD simulations [64]. The thermal conductivity was found to be dependent on length, temperature and temperature "boundary" condition, and a significantly suppressed for the shorter lengths. Xu et al. [65] fabricated the single-walled carbon nanotube (SWNT)-poly vinylidene fluoride (PVDF) composites by dispersion of SWNT in an aqueous surfactant solution, followed by mixing with PVDF powder, filtration and hot pressing, and 19.3% increase in the thermal conductivity of the composite was reported by addition of 5% (by volume) CNT.

Nishimura and Liu [66] used boundary integral equation (BIE) formulation for the thermal analysis of CNT based nano-composites. They solved the heat conduction problems in 2-D infinite domain embedded with many rigid inclusions with the help of a fast multipole boundary element method using continuum mechanics approach. Zhang et al. [67–69] used a continuum mechanics based meshless hybrid boundary node method (hybrid BNM) for the heat conduction analysis of CNT based nano-composites. They used multi-domain and simplified approaches coupled with fast multipole method to solve large scale problems. In their study, they found that by addition of 7.2% (by volume) of CNTs in the polymer matrix results in an increase of 49% in the thermal conductivity of the composite.

At nanoscale, experiments are very difficult to conduct and currently molecular level simulations of CNTs and CNT based composites are limited to very small length and time scales, and cannot deal with the large scale problems. For real engineering applications, nano-composites must expand from nano to micro, and ultimately to macro length scales. Therefore, continuum mechanics models can play a significant role in the analysis of these composites. Till date, the validity of continuum mechanics approach for the modeling of CNT based composites is not fully-established, and it will be questioned for some time to come. However, at present, it seems to be the only feasible approach for the large scale simulation of CNT-based composites. The best argument for using continuum approach in the present simulation is that it has been applied successfully by many researchers for studying the mechanical, electrical and thermal properties of CNTs and CNT reinforced composites [41–55, 66–69]. In these studies, CNTs were treated as homogeneous and isotropic materials using continuum beam, shell, 3-D space frames as well as 3-D solid models. The various issues related to the modeling of CNT-based composites using continuum approach have been discussed by Liu and Chen [43]. They proposed the 3-D elasticity models, instead of frame, beam or shell models for modeling the CNTs embedded in a matrix. They also proposed three kinds of representative volume elements (RVEs) namely cylindrical RVE, square RVE and hexagonal RVE for the modeling of CNT based composites.

So far, only boundary type methods (BEM and hybrid BNM) were applied to predict the thermal behavior of CNT based composites using continuum mechanics approach. In BEM and hybrid BNM, square representative volume element (square RVE) was used to obtain the thermal properties of the nano-composites, but these methods do not have symmetry, bandedness and sparseness properties in their solution matrix; therefore, the solution of large scale problems is relatively tedious and expensive task as compared to domain type methods such as finite element method (FEM) and element free Galerkin (EFG) method. Both FEM and EFG method possess all these properties in their solution matrix. Although, FEM is the most general method in the category of domain type methods, but it has not been used in the present work due to its problem in discretization of complex domain into elements. To alleviate the problems faced by FEM, domain type meshless EFG method has been used in the present work to evaluate the thermal properties of CNT based nano-composites. Numerical results have been obtained by cylindrical representative volume element (cylindrical RVE) using continuum mechanics approach. The equivalent thermal conductivity has been plotted as function of nanotube length, nanotube radius, RVE length and RVE radius. An approximate formula is proposed to evaluate the equivalent thermal conductivity of CNT based composites. The values of equivalent heat conductivity, obtained by simplified approach have been found in good conformity with those obtained by multi-domain approach.

2 Review of element free Galerkin (EFG) method

The EFG method requires moving least square (MLS) approximants for the discretization of the governing equations. These MLS approximants consist of three components: a weight function associated with each node, a basis function and a set of constant coefficients that depends on position. Using MLS approximation scheme, an unknown function of temperature $T(\mathbf{r})$ is approximated as $T^h(\mathbf{r})$ [70].

$$T^h(\mathbf{r}) = \sum_{j=1}^{m} p_j(\mathbf{r}) a_j(\mathbf{r}) = \mathbf{p}^{\mathrm{T}}(\mathbf{r})\,\mathbf{a}(\mathbf{r}), \tag{1}$$

where, $\mathbf{r}^{\mathrm{T}} = [r \quad z]$, $\mathbf{p}^{\mathrm{T}}(\mathbf{r}) = \begin{bmatrix} 1 & r & z \end{bmatrix}$, $m = 3$ and $\mathbf{a}^{\mathrm{T}}(\mathbf{r}) = [a_1(\mathbf{r}),\ a_2(\mathbf{r}),\ a_3(\mathbf{r})]$

The unknown coefficients $\mathbf{a}(\mathbf{r})$ at any given point are determined by minimizing the functional J.

$$J = \sum_{I=1}^{n} w(\mathbf{r} - \mathbf{r}_I)[\mathbf{p}^{\mathrm{T}}(\mathbf{r})\,\mathbf{a}(\mathbf{r}) - T_I]^2, \tag{2}$$

where, n is the number of nodes in the neighborhood of $\mathbf{r}$ for which the weight function $w(\mathbf{r} - \mathbf{r}_I) \neq 0$ and T_I is the nodal

parameter at $\mathbf{r} = \mathbf{r}_I$. The stationary value of J in Eq. (2) w.r.t $\mathbf{a}(\mathbf{r})$ leads to the following set of linear equations

$$\mathbf{a}(\mathbf{r}) = \mathbf{A}^{-1}(\mathbf{r})\mathbf{B}(\mathbf{r})\mathbf{T}. \tag{3}$$

where,

$$\mathbf{A}(\mathbf{r}) = w(\mathbf{r}-\mathbf{r}_1)\begin{bmatrix} 1 & r_1 & z_1 \\ r_1 & r_1^2 & r_1 z_1 \\ z_1 & r_1 z_1 & z_1^2 \end{bmatrix} + \cdots + w(\mathbf{r}-\mathbf{r}_n)\begin{bmatrix} 1, & r_n & z_n \\ r_n & r_n^2 & r_n z_n \\ z_n & r_n z_n & z_n^2 \end{bmatrix} \tag{4}$$

$$\mathbf{B}(\mathbf{r}) = \left\{ w(\mathbf{r}-\mathbf{r}_1)\begin{bmatrix} 1 \\ r_1 \\ z_1 \end{bmatrix}, w(\mathbf{r}-\mathbf{r}_2)\begin{bmatrix} 1 \\ r_2 \\ z_2 \end{bmatrix}, \cdots w(\mathbf{r}-\mathbf{r}_n)\begin{bmatrix} 1 \\ r_n \\ z_n \end{bmatrix} \right\} \tag{5}$$

$$\mathbf{T}^{\mathrm{T}} = [T_1, T_2, T_3, \cdots T_n]. \tag{6}$$

By substituting Eq. (3) in Eq. (1), the MLS approximants can be written as

$$\begin{aligned} T^h(\mathbf{r}) &= \mathbf{p}^{\mathrm{T}}(\mathbf{r})\mathbf{A}^{-1}(\mathbf{r})\mathbf{B}(\mathbf{r})\mathbf{T} \\ &= \sum_{I=1}^{n}\sum_{j=1}^{m} p_j(\mathbf{r})(\mathbf{A}^{-1}(\mathbf{r})\mathbf{B}(\mathbf{r}))_{jI} \\ &= \sum_{I=1}^{n} \Phi_I(\mathbf{r})\, T_I \\ &= \Phi(\mathbf{r})\,\mathbf{T}, \end{aligned} \tag{7}$$

where T_I are the nodal parameters and $\Phi_I(\mathbf{r})$is the shape function, which is defined as

$$\Phi_I(\mathbf{r}) = \sum_{j=1}^{m} p_j(\mathbf{r})(\mathbf{A}^{-1}(\mathbf{r})\mathbf{B}(\mathbf{r}))_{jI} = \mathbf{p}^{\mathrm{T}}\mathbf{A}^{-1}\mathbf{B}_I. \tag{8}$$

2.1 Weight function description

The weight function $w(\mathbf{r}-\mathbf{r}_I)$ is non-zero over a small neighborhood of $\mathbf{r}_I$, called the domain of influence of node I. The choice of weight function $w(\mathbf{r}-\mathbf{r}_I)$ affects the resulting approximation $T^h(\mathbf{r}_I)$, therefore, exponential weight function [71] has been used in the present work, which is given as

$$w(s) = \begin{Bmatrix} C^{-s} & 0 \le s \le 1 \\ 0 & s > 1 \end{Bmatrix}, \tag{9}$$

where $1,000 \le C \le 5,000$, $s = \frac{||\mathbf{r}-\mathbf{r}_I||}{d_{mI}}$ is the normalized radius, $(s_r)_I = \frac{||r-r_I||}{d_{mrI}}$, $(s_z)_I = \frac{||z-z_I||}{d_{mzI}}$, $d_{mI} = d_{\max} c_I$, $d_{mrI} = d_{\max} c_{rI}$, $d_{mzI} = d_{\max} c_{zI}$, $\|\mathbf{r}-\mathbf{r}_I\|$ is the distance between evaluation points and nodal points, $d_{\max}$= scaling parameter, c_{rI} and c_{zI} at node I are the distances to the nearest neighbors.

3 Numerical implementation

Carbon nanotubes (CNTs) possess very high value of thermal conductivity as compared to polymer matrix in CNT based composites. This unusually high value of thermal conductivity makes them to behave as a superconductor. During thermal analysis of CNT based composites, Zhang et al. [67] found that the temperature distribution on the surface of CNTs comes out to be almost uniform. They used the simplified approach in their further work [69], and obtained the thermal properties by assuming CNT surface at a constant temperature [68] using square RVE. In the present work, cylindrical RVE has been used for the thermal analysis of nano-composites. A perfect bonding has been assumed between the nanotube material and polymer matrix. Both multi-domain and simplified approaches have been used, and compared with each other. In multi-domain approach, both matrix and CNT have been discretised, whereas in simplified approach, only matrix domain has been modeled. In simplified approach, CNT surface is assumed at an unknown constant temperature. A model containing single CNT inside cylindrical RVE has been taken to obtain the thermal properties. Both ends of RVE are subjected to constant temperatures and outer surface is kept insulated. This problem has been solved by treating it an axisymmetric heat transfer problem, governed by the steady sate heat conduction equation in cylindrical coordinate system. The governing heat conduction equation can be written as

$$k_r \frac{\partial^2 T}{\partial r^2} + \frac{k_r}{r}\frac{\partial T}{\partial r} + k_z \frac{\partial^2 T}{\partial z^2} = 0 \tag{10a}$$

with the following essential boundary conditions

$$\text{at } z = 0, \quad T = T_{\mathrm{L}} \tag{10b}$$

$$\text{at } z = L, \quad T = T_{\mathrm{R}}. \tag{10c}$$

The above equation can be re-written as

$$\frac{1}{r}\frac{\partial}{\partial r}\left(k\, r \frac{\partial T}{\partial r}\right) + \frac{\partial}{\partial z}\left(k \frac{\partial T}{\partial z}\right) = 0, \tag{11}$$

where $k_r = k_z = k$.

3.1 Multi-domain approach

Both polymer matrix and nanotube have been modeled in multi-domain approach. To evaluate the properties using multi-domain approach, the selected modeling parameters along with boundary conditions are given in Fig. 1. The compatibility requirement at the interface of matrix and CNT is given by

$$q|_{\mathrm{m}_1} = q|_{\mathrm{m}_2}\,, \tag{12}$$

where $q|_{m_1}$and $q|_{m_2}$are the value of heat fluxes at the interface.

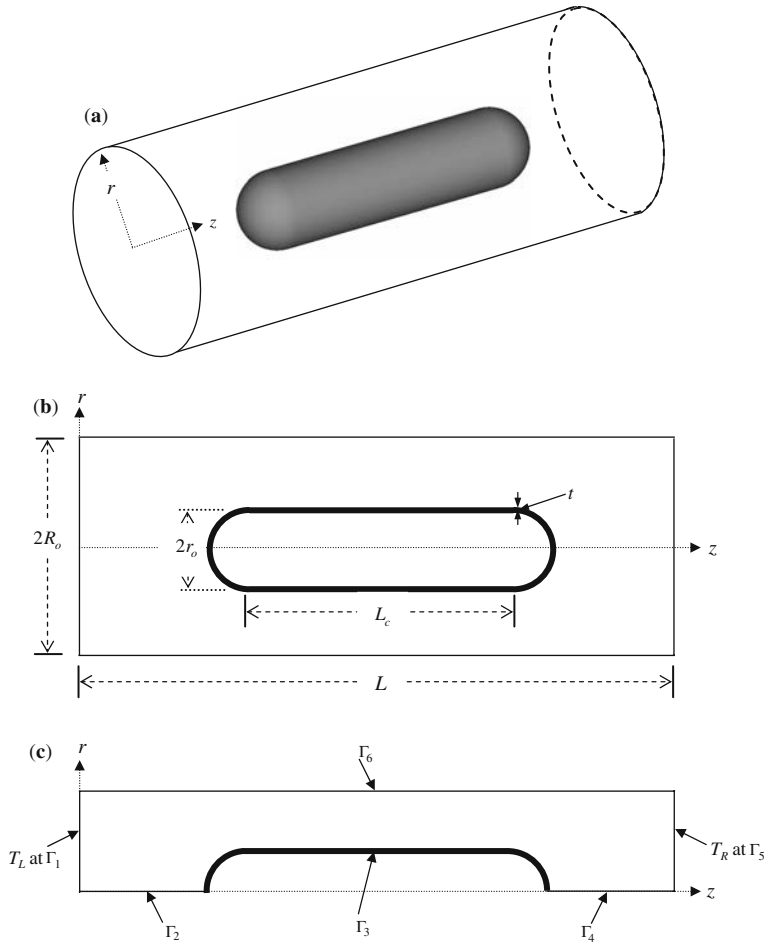

Fig. 1 Model for CNT problem **a** nanoscale cylindrical representative volume element containing single nanotube, **b** dimensions of the model and **c** computational model with boundary conditions

Using divergence theorem, the weak form of the Eq. (11) is obtained as

$$2\pi \sum_{i=m_1,m_2} \int_{\Omega_i} \left(k_i \frac{\partial \bar{w}}{\partial r} \frac{\partial T}{\partial r} + k_i \frac{\partial \bar{w}}{\partial z} \frac{\partial T}{\partial z} \right) r \, \mathrm{d}r \, \mathrm{d}z - 2\pi \sum_{i=m_1,\, m_2} \int_{\Gamma} \bar{w} \, r \, q_i \, \mathrm{d}\Gamma = 0, \tag{13}$$

where $q_i = k_i \frac{\partial T}{\partial r} \cos(n', r) + k_i \frac{\partial T}{\partial z} \cos(n', z)$, k_{m_1} and k_{m_2} are the values of thermal conductivity of the matrix and CNT, respectively.

The functional $I(T)$can be written as

$$I(T) = \pi \sum_{i=m_1,m_2} \int_{\Omega_i} k_i \left[\left(\frac{\partial T}{\partial r} \right)^2 + \left(\frac{\partial T}{\partial z} \right)^2 \right] r \, \mathrm{d}r \, \mathrm{d}z. \tag{14}$$

Enforcing essential boundary conditions using penalty method, the functional $I^*(T)$ is obtained as

$$I^*(T) = \pi \sum_{i=m_1,m_2} \int_{\Omega_i} k_i \left[\left(\frac{\partial T}{\partial r} \right)^2 + \left(\frac{\partial T}{\partial z} \right)^2 \right] r \, \mathrm{d}r \, \mathrm{d}z + \frac{\alpha}{2} \int_{\Gamma_1} (T - T_L)^2 \mathrm{d}\Gamma + \frac{\alpha}{2} \int_{\Gamma_5} (T - T_R)^2 \mathrm{d}\Gamma. \tag{15}$$

Taking variation, i.e. $\delta\, I^*(T)$ of Eq. (15), it reduces to

$$\delta\, I^*(T) = 2\pi \sum_{i=m_1,m_2} \int_{\Omega_i} k_i \left[\left(\frac{\partial T}{\partial r} \right)^{\mathrm{T}} \delta \left(\frac{\partial T}{\partial r} \right) + \left(\frac{\partial T}{\partial z} \right)^{\mathrm{T}} \delta \left(\frac{\partial T}{\partial z} \right) \right] r \, \mathrm{d}r \mathrm{d}z + \alpha \int_{\Gamma_1} (T - T_L) \delta T \, \mathrm{d}\Gamma + \alpha \int_{\Gamma_5} (T - T_R) \delta T \, \mathrm{d}\Gamma, \tag{16}$$

where α is the penalty parameter.

Since $\delta I^*(T) = 0$ and δT are arbitrary in Eq. (16), a following set of equations is obtained using Eq. (7)

$$[\mathbf{K}]\{T\} = \{\mathbf{f}\}, \tag{17a}$$

where

$$K_{IJ} = 2\pi \sum_{i=m_1,m_2} \int_{\Omega_i} \begin{bmatrix} \Phi_{I,r} \\ \Phi_{I,z} \end{bmatrix}^{\mathrm{T}} \begin{bmatrix} k_i & 0 \\ 0 & k_i \end{bmatrix} \begin{bmatrix} \Phi_{I,r} \\ \Phi_{I,z} \end{bmatrix} r\,\mathrm{d}r\mathrm{d}z + \alpha \int_{\Gamma_1} \Phi_I\,\Phi_J \mathrm{d}\Gamma + \alpha \int_{\Gamma_5} \Phi_I\,\Phi_J \mathrm{d}\Gamma \tag{17b}$$

$$f_I = \alpha \int_{\Gamma_1} T_L \Phi_I \mathrm{d}\Gamma + \alpha \int_{\Gamma_5} T_R \Phi_I \mathrm{d}\Gamma. \tag{17c}$$

Equation (17a) represents a symmetric, sparse system of linear equations, which is solved by direct method using Matlab functions.

3.2 Simplified approach

In simplified approach, only matrix domain has been modeled, since CNT is assumed at a constant (unknown) temperature. The numerical formulation of the this problem using simplified approach is given by the following steps:

Using divergence theorem, the weak form of Eq. (11) is obtained as

$$2\pi \int_{\Omega_1} \left(k_{m_1} \frac{\partial \bar{w}}{\partial r} \frac{\partial T}{\partial r} + k_{m_1} \frac{\partial \bar{w}}{\partial z} \frac{\partial T}{\partial z} \right) r\,\mathrm{d}r\,\mathrm{d}z - 2\pi \int_{\Gamma} \bar{w}\, r\, q\, \mathrm{d}\Gamma = 0, \tag{18}$$

where $q = k_{m_1} \frac{\partial T}{\partial r} \cos(n', r) + k_{m_1} \frac{\partial T}{\partial z} \cos(n', z)$.

The functional $I(T)$ can be obtained as

$$I(T) = 2\pi \int_{\Omega_1} \frac{1}{2} k_{m_1} \left[\left(\frac{\partial T}{\partial r} \right)^2 + \left(\frac{\partial T}{\partial z} \right)^2 \right] r\,\mathrm{d}r\,\mathrm{d}z. \tag{19}$$

Enforcing essential boundary conditions using penalty method, the functional $I^*(T)$ is obtained as

$$I^*(T) = 2\pi \int_{\Omega_1} \frac{1}{2} k_{m_1} \left[\left(\frac{\partial T}{\partial r} \right)^2 + \left(\frac{\partial T}{\partial z} \right)^2 \right] r\,\mathrm{d}r\,\mathrm{d}z + \frac{\alpha}{2} \int_{\Gamma_1} (T - T_L)^2 \mathrm{d}\Gamma + \frac{\alpha}{2} \int_{\Gamma_5} (T - T_R)^2 \mathrm{d}\Gamma. \tag{20}$$

Taking variation, i.e. $\delta I^*(T)$ of Eq. (20), it reduces to

$$\delta I^*(T) = 2\pi \int_{\Omega_1} k_{m_1} \left[\left(\frac{\partial T}{\partial r} \right)^{\mathrm{T}} \delta \left(\frac{\partial T}{\partial r} \right) + \left(\frac{\partial T}{\partial z} \right)^{\mathrm{T}} \delta \left(\frac{\partial T}{\partial z} \right) \right] r\,\mathrm{d}r\mathrm{d}z + \alpha \int_{\Gamma_1} (T - T_L) \delta T\, \mathrm{d}\Gamma + \alpha \int_{\Gamma_5} (T - T_R) \delta T\, \mathrm{d}\Gamma. \tag{21}$$

Since $\delta I^*(T) = 0$ and δT are arbitrary in Eq. (21), a following set of equations is obtained using Eq. (7)

$$[\mathbf{K}]\{T\} = \{\mathbf{f}\}, \tag{22a}$$

where

$$K_{IJ} = 2\pi \int_{\Omega_1} \begin{bmatrix} \Phi_{I,r} \\ \Phi_{I,z} \end{bmatrix}^{\mathrm{T}} \begin{bmatrix} k_{m_1} & 0 \\ 0 & k_{m_1} \end{bmatrix} \begin{bmatrix} \Phi_{I,r} \\ \Phi_{I,z} \end{bmatrix} r\,\mathrm{d}r\mathrm{d}z + \alpha \int_{\Gamma_1} \Phi_I\,\Phi_J \mathrm{d}\Gamma + \alpha \int_{\Gamma_5} \Phi_I\,\Phi_J \mathrm{d}\Gamma \tag{22b}$$

$$f_I = \alpha \int_{\Gamma_1} T_L \Phi_I \mathrm{d}\Gamma + \alpha \int_{\Gamma_5} T_R \Phi_I \mathrm{d}\Gamma. \tag{22c}$$

Since CNT surface is assumed at an unknown constant temperature, hence Eq. (22a) is re-written as

$$\begin{bmatrix} \mathbf{K}_{pp} & \mathbf{K}_{pq} \\ \mathbf{K}_{qp} & \mathbf{K}_{qq} \end{bmatrix} \begin{Bmatrix} \mathbf{T}_p \\ \mathbf{T}_q \end{Bmatrix} = \begin{Bmatrix} \mathbf{f}_p \\ \mathbf{f}_q \end{Bmatrix}, \tag{23a}$$

where

$$(f_P)_I = \alpha \int_{\Gamma_1} T_L \Phi_I \mathrm{d}\Gamma + \alpha \int_{\Gamma_5} T_R \Phi_I \mathrm{d}\Gamma \tag{23b}$$

$$(f_q)_I = \alpha \int_{\Gamma_3} T_{\mathrm{C}}\, \Phi_I \mathrm{d}\Gamma \tag{23c}$$

$$\begin{bmatrix} \mathbf{K}_{pp} & \mathbf{K}_{pq} \\ \mathbf{K}_{qp} & \mathbf{K}_{qq} \end{bmatrix} = [\bar{\mathbf{K}}] \text{with} \bar{K}_{IJ} = K_{IJ} + \alpha \int_{\Gamma_3} \Phi_I\,\Phi_J \mathrm{d}\Gamma. \tag{23d}$$

$\mathbf{T}_q$ and $\mathbf{T}_p$ are the values of temperature degree of freedom on CNT surface and rest of the matrix-domain, respectively.

The Eq. (23a) is further written as

$$\begin{bmatrix} \mathbf{K}_{pp} & \mathbf{K}_{pq} \\ \mathbf{K}_{qp} & \mathbf{K}_{qq} \end{bmatrix} \begin{Bmatrix} \mathbf{T}_p \\ \mathbf{T}_q \end{Bmatrix} = \begin{Bmatrix} \mathbf{f}_p \\ \mathbf{f}'_q\, T_{\mathrm{C}} \end{Bmatrix}, \tag{24}$$

where T_{C} is the constant temperature on the CNT surface and $(f'_q)_I = \alpha \int_{\Gamma_3} \Phi_I \mathrm{d}\Gamma$.

Now in Eq. (24), there is one additional unknown which needs one more equation to solve the system of equations. This additional equation is obtained using law of conservation of energy at the CNT surface, i.e. (net rate of thermal energy flowing through CNT surface is zero):

$$\int_{\Gamma_3} q \mathrm{d}\Gamma = 0. \tag{25}$$

Introducing Eq. (25) in Eq. (24), it takes the following form

$$\left[\begin{array}{cc|c} \mathbf{K}_{pp} & \mathbf{K}_{pq} & 0 \\ \mathbf{K}_{qp} & \mathbf{K}_{qq} & -\mathbf{f}'_q \\ \hline 0 & \mathbf{f}''_q & 0 \end{array}\right] \begin{Bmatrix} \mathbf{T}_p \\ \mathbf{T}_q \\ T_{\mathrm{C}} \end{Bmatrix} = \begin{Bmatrix} \mathbf{f}_p \\ 0 \\ 0 \end{Bmatrix}, \tag{26}$$

where $(f_q'')_I = \int_{\Gamma_3} \frac{\mathrm{d}\Phi}{\mathrm{d}n'}\mathrm{d}\Gamma$ with n' is the outward normal to the surface.

Equation (26) represents a non-symmetric, sparse system of linear equations, which is solved by direct method using Matlab functions.

4 Results and discussion

In this section, a model CNT based composite problem has been solved using multi-domain and simplified approaches. A nanoscale cylindrical representative volume element containing single nanotube is shown in Fig. 1a, and its dimensions are shown in Fig. 1b. The computational model along with boundary conditions is shown in Fig. 1c. To evaluate the equivalent thermal conductivity of the composite, two ends of RVE are maintained at two different constant temperatures, and outer cylindrical surface is kept insulated. Carbon nanotube is placed symmetrically at the center of RVE such that the axis of RVE is coinciding with the axis of CNT. The data used for the model problem (as shown in Fig. 1) is tabulated in Table 1. Dimensions and properties for the model have been chosen from a wide range available in literature [66–69]. Polycarbonate [68, 69] has been taken as matrix material for the composite. The EFG results have been obtained using uniform nodal data distribution scheme for 2,501 nodes. In both multi-domain and simplified approaches, same numbers of nodes, i.e. (2,501 nodes) have been taken inside polymer matrix for a fair comparison of EFG results. The EFG results not only depend upon the weight function but also depend on the support size [72], therefore, a value of support size, i.e. $d_{\max}$= 1.21 has been chosen from a prescribed range of scaling parameter for heat transfer applications [72]. The codes have been written in Matlab to obtain the EFG results for both multi-domain and simplified approaches.

Assuming material properties as homogeneous, isotropic and independent of temperature, the equivalent thermal conductivity of the composite has been evaluated as

$$k_{\mathrm{e}} = -\frac{q\,L}{\Delta T}, \tag{27}$$

where k_{e}denotes the equivalent thermal conductivity of the composite, L is the length of RVE, $q$is normal heat flux density and $\Delta T$is the temperature difference between two ends of RVE.

The percentage volume fraction of CNT [67] has been calculated by the following expression

$$v = \left(\frac{V_{m_1}}{V_{m_1} + V_{m_2}}\right) \times 100, \tag{28}$$

where v is the volume fraction of CNT in composite, $V_{m_1}$is the volume of polymer matrix and $V_{m_2}$is the volume of CNT including cavity. The cavity has been considered a part of the nanotube for the calculation of volume fraction (v) only, since the addition of a nanotube inside RVE occupies the volume required by nanotube including cavity.

In the present work, an approximate formula is proposed to evaluate the equivalent thermal conductivity of the composite:

$$k_{\mathrm{e}} = k_{m_1}\left(\frac{L}{L + 1.55R_o - 1.04L_c - 3.55r_o}\right), \tag{29}$$

where k_{e}= equivalent thermal conductivity of the nano-composite, k_{m_1}= thermal conductivity of the polymer matrix, L= RVE length, R_o= radius of cylindrical RVE, L_c= nanotube length and r_o= nanotube outer radius.

Zhang et al. [67] also proposed an approximate formula to evaluate the equivalent thermal conductivity of CNT composites:

$$k_{\mathrm{e}} = k_{m_1}\left(\frac{L}{L - L_c - 0.4r_o}\right). \tag{30}$$

Table 1 Data for CNT based composite problem

Parameters	Value of parameters
RVE length (L)	100 nm
Nanotube length (L_c)	50 nm
RVE radius (R_o)	12 nm
Nanotube outer radius (r_o)	5 nm
Nanotube thickness (t)	0.4 nm
Thermal conductivity of polymer matrix (k_{m_1})	0.37 W/m K
Thermal conductivity of nanotube (k_{m_2})	6,000 W/m K
Penalty parameter (α)	10^3
Temperature at $\Gamma_1(T_L)$	300 K
Temperature at $\Gamma_5(T_R)$	100 K

4.1 Temperature variation with RVE length (L)

The data required for the study of temperature with RVE length, is presented in Table 1. The temperature values obtained using multi-domain and simplified approaches are presented in Fig. 2 at location r = 5.175 nm. From the results

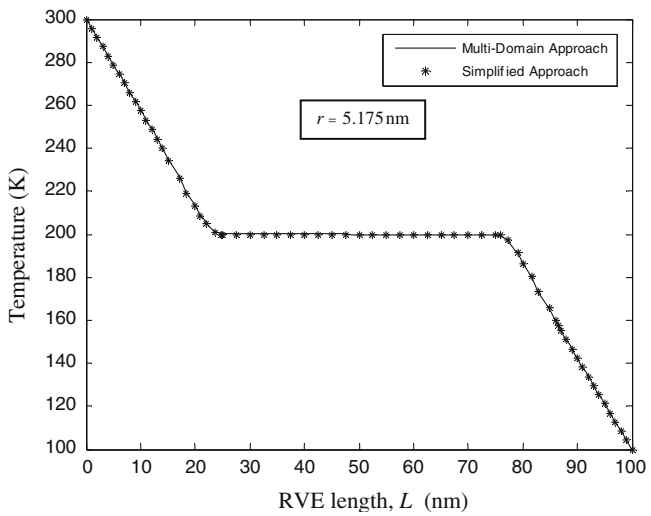

Fig. 2 Variation of temperature with RVE length (L)

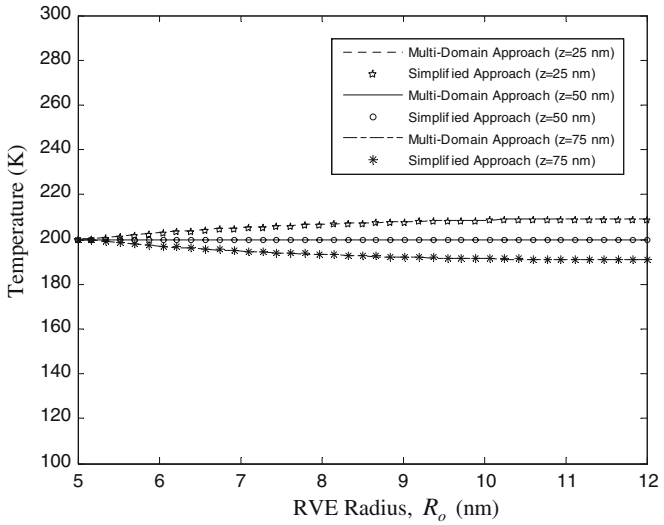

Fig. 3 Variation of temperature with RVE Radius (R_o)

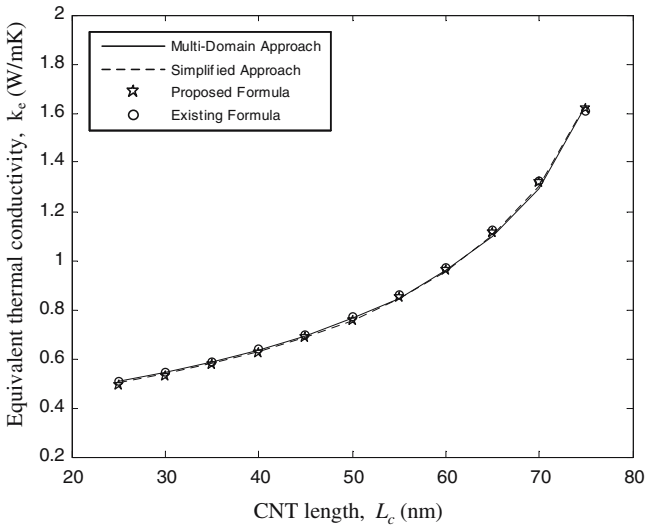

Fig. 4 Variation of equivalent thermal conductivity (k_e) with CNT length (L_c)

presented in Fig. 2, it has been observed that the temperature first decreases rapidly from left cylindrical face (300 K) to the left end of CNT (200 K) after that it remains almost constant (200 K) along CNT length near the CNT surface then it again decreases from right end of CNT (200 K) to 100 K. This behavior of temperature show that the most of the heat flux passes through the nanotube only. The results obtained by simplified approach have been found in good conformity with multi-domain approach.

4.2 Temperature variation with RVE radius (r_o)

The variation of temperature with RVE radius has also been studied for the same data as presented in Table 1. The values of temperature, obtained using multi-domain and simplified approaches are presented in Fig. 3 at three different locations, i.e. $z = 25, 50$ and 75 nm. From the results presented in Fig. 3, it can be noted that the temperature remains almost constant for $z = 50$ nm from $r = 5$ to 12 nm whereas for $z = 25$ nm, there is a gradual increase in the value of temperature with the increase of r and for $z = 75$ nm, temperature decreases gradually with increase of r. These observations also show that the most of the heat flux passes through the nanotube portion of the composite. Moreover, the results obtained by simplified and multi-domain approaches have been found almost similar with each other.

4.3 Effect of CNT length (L_c) on equivalent thermal conductivity (k_e)

This sub-section describes the effect of CNT length on the equivalent thermal conductivity of the composites. The various parameters required for this analysis are given in Table 1. The values of thermal conductivity have been evaluated by both multi-domain and simplified approaches. Various values of CNT length (from 25 to 75 nm) have been taken to study the effect of CNT length on thermal conductivity. Figure 4 shows the variation of equivalent thermal conductivity with CNT length. For $L_c = 25$ nm (5.5% by volume), the values of equivalent thermal conductivities obtained by multi-domain and simplified approaches are found to be 0.5066 and 0.5040 W/m K, respectively, whereas for $L_c = 75$ nm (14.2% by volume), the values of thermal conductivities are found to be 1.6258 and 1.6334 W/m K, respectively. The results obtained by simplified and multi-domain approaches are also compared with those obtained by proposed and existing formulas and has been found in good concurrence with them.

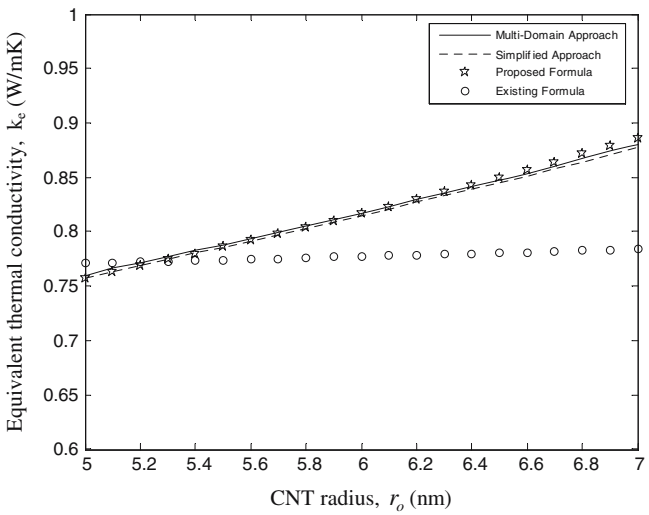

Fig. 5 Variation of equivalent thermal conductivity (k_e) with CNT radius (r_o)

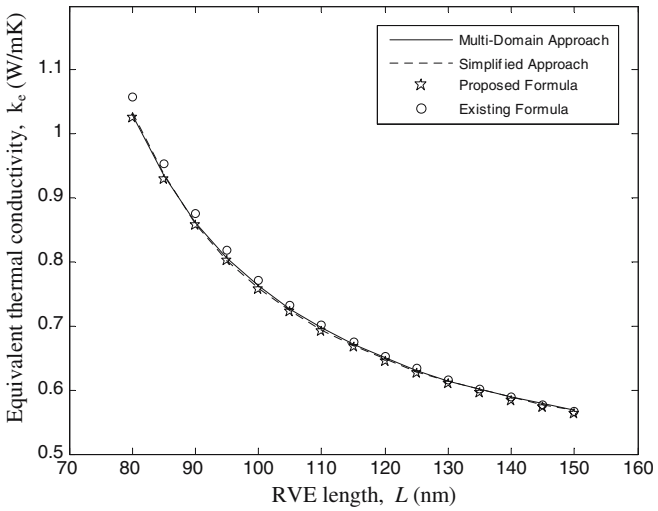

Fig. 6 Variation of equivalent thermal conductivity (k_e) with RVE length (L)

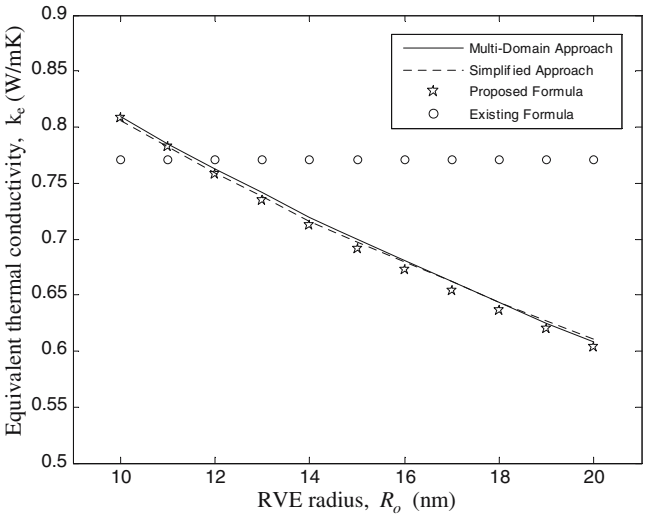

Fig. 7 Variation of equivalent thermal conductivity (k_e) with RVE radius (R_o)

4.4 Effect of CNT radius (r_o) on equivalent thermal conductivity (k_e)

In this sub-section, the EFG results have been obtained using different values of CNT radius for L_c= 50 nm. The equivalent thermal conductivity has been evaluated by multi-domain approach, simplified approach, proposed approximate formula and existing approximate formula for various values of CNT radius and is shown in Fig. 5. From the results presented in Fig. 5, it can be concluded that the results obtained by EFG method using multi-domain and simplified approaches are almost similar with those obtained by proposed formula. The results obtained by existing formula, proposed by Zhang et al. [67] are insignificant for this study since they proposed their formula mainly by taking the effect CNT length on equivalent thermal conductivity of the composite. They did not even analyze the effect of CNT radius (r_o) on the equivalent thermal conductivity of the composite.

4.5 Effect of RVE length (L) on equivalent thermal conductivity (k_e)

Various values of RVE length (from 80 to 150 nm) have been taken to study the effect of RVE length on the equivalent thermal conductivity of the composites. Fig. 6 shows the variation of equivalent thermal conductivity with RVE length. The values of equivalent thermal conductivities, obtained by multi-domain and simplified approaches are 2.78 and 2.79 times that of polymer matrix, respectively, for L= 80 nm i.e. (12.3% by volume) whereas for L= 150 nm i.e. (6.5% by volume), the values of equivalent thermal conductivity are 1.54 times that of polymer matrix using both approaches. The results obtained by EFG method using multi-domain and simplified approaches are also compared with those obtained by proposed and existing formulas and have been found in good agreement among themselves.

4.6 Effect of RVE radius (R_o) on equivalent thermal conductivity (k_e)

This sub-section describes the effect of RVE radius (R_o) on equivalent thermal conductivity of the composite. The values of thermal conductivity obtained by different techniques are shown in Fig. 7 for various values of RVE radius. The values of the equivalent thermal conductivities obtained by multi-domain approach, simplified approach, proposed formula and existing formula are 0.8088, 0.8085, 0.8087 and 0.7708 W/m K, respectively, for R_c = 10 nm, i.e. (14.2% by volume), whereas the values of $k_e$obtained by these methods are 0.6084, 0.6100, 0.6041 and 0.7708 W/m K, respectively, for R_c = 20 nm, i.e. (3.5% by volume). From the results presented in Fig. 7, it can be noted that the thermal conductivity decreases with the increase in RVE radius for multi-domain approach, simplified approach and proposed formula whereas in existing formula, thermal conductivity has been considered independent of RVE radius. The present simulation clearly shows that the equivalent thermal conductivity is a function RVE radius.

4.7 Computational cost

In this sub-section, a comparison of computational cost, i.e. (CPU time) have been made for both multi-domain and simplified approaches. Same number of nodes has been taken inside polymer matrix for a fair comparison of CPU time between two approaches. The CPU time has been obtained on a Dell machine (2.0 GHz Processor and 1 GB Ram) using Matlab codes. The average CPU time required by multi-domain and simplified approaches has been plotted in Fig. 8 for various values of data size, i.e. (number of nodes). From Fig. 8, a significant difference has been observed in the CPU time required by the two approaches. The CPU time required by multi-domain approach is more as compared to the CPU

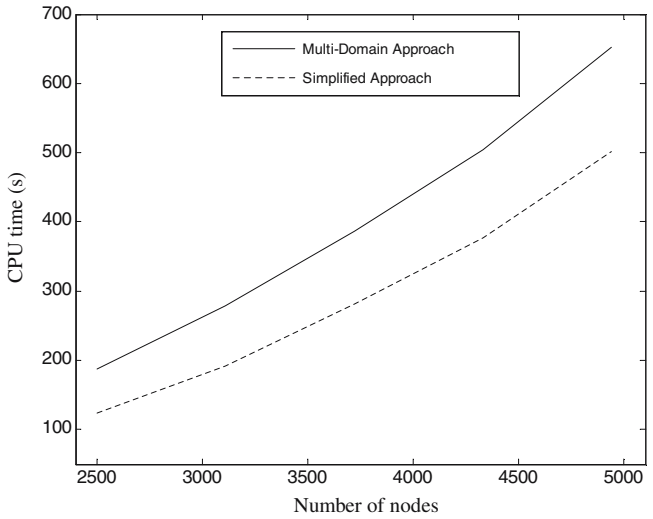

Fig. 8 Variation of CPU time with data size, i.e. (number of nodes)

time required by simplified approach for the same data size, i.e. (number of nodes), since in multi-domain approach, both matrix and nanotube have been modeled, whereas in case of simplified approach, only matrix domain has been modeled. Moreover, difference between CPU times for two-approaches goes on increasing with the increase of data size.

5 Conclusions

In this work, an initial step has been made to evaluate the thermal properties of CNT based composites by element free Galerkin method. The equivalent thermal conductivity has been calculated using continuum approach and plotted with various model parameters. Both multi-domain and simplified approaches have been applied and compared with each other. Present computations show that thermal conductivity of the composites is a function of CNT length, CNT radius, RVE length and RVE radius. An approximate formula has been proposed to evaluate the equivalent thermal conductivity of nano-composites. The results obtained by simplified approach and proposed formula have been found in good agreement with those obtained by multi-domain approach. Due to accuracy and capability of handling complicated geometries, the element free Galerkin method with simplified approach can be extended to predict the thermal properties of CNT-composites having arbitrary shaped CNTs randomly distributed in the polymer matrix.

Acknowledgements This work was supported by the CLUSTER of Ministry of Education, Culture, Sports, Science and Technology, Japan.

References

1. Thostensona ET, Renb Z, Chou TW (2001) Advances in the science and technology of carbon nanotubes and their composites: a review. Composites Sci Technol 61:1899–1912
2. Dai H (2002) Carbon nanotubes: opportunities and challenges. Surface Sci 500:218–241
3. Bernholc J, Brenner D, Buongiorno Nardelli M, Meunier V, Roland C (2002) Mechanical and electrical properties of nanotubes. Ann Rev Mater Res 32:347–375
4. Qian D, Wagner GJ, Liu WK, Yu MF, Ruoff RS (2002) Mechanics of carbon nanotubes. Appl Mech Rev 55:495–532
5. Breuer O, Sundararaj U (2004) Big returns from small fibers: a review of polymer/carbon nanotube composites. Polym Composite 25:630–645
6. Popov VN (2004) Carbon nanotubes: properties and application. Mater Sci Eng R Rep 43:61–102
7. Harris PJF (2004) Carbon nanotube composites. Int Mater Rev 49:31–43
8. Rafii-Tabar H (2004) Computational modelling of thermo-mechanical and transport properties of carbon nanotubes. Phy Rep 390:235–452
9. Shen S, Atluri SN (2004) Computational nano-mechanics and multi-scale simulation. Comput Mater Continua 1:59–90
10. Khare R, Bose S (2005) Carbon nanotube based composites- a review. J Miner Mater Characterization Eng 4:31–46
11. Treacy MMJ, Ebbesen TW, Gibson JM (1996) Exceptionally high Young's modulus observed for individual carbon nanotubes. Nature 381:678–680
12. Krishnan A, Dujardin E, Ebbesen TW, Yianilos PN, Treacy MMJ (1998) Young's modulus of single-walled nanotubes. Phys Rev B 58:14013–14019
13. Salvetat JP, Briggs GAD, Bonard JM, Bacsa RR, Kulik AJ, Stöckli T, Burnham NA, Forr'o L (1999) Elastic and shear moduli of single-walled carbon nanotube ropes. Phys Rev Lett 82:944–947
14. Salvetat JP, Kulik AJ, Bonard JM, Briggs GAD, Stöckli T, M'et'enier K, Bonnamy S, B'eguin F, Burnham NA, Forr'o L (1999) Elastic modulus of ordered and disordered multiwalled carbon nanotubes. Adv Mater 11:161–165
15. Salvetat JP, Bonard JM, Thomson NH, Kulik AJ, Forro L, Benoit W, Zuppiroli L (1999) Mechanical properties of carbon nanotubes. Appl Phys A 69:255–260
16. Jia Z, Wang Z, Xu C, Liang J, Wei B, Wu D, Zhu S (1999) Study on poly (methyl methacrylate): carbon nanotube composites. Mater Sci Eng A 271:395–400
17. Xie S, Li W, Pan Z, Chang B, Sun L (2000) Mechanical and physical properties on carbon nanotube. J Phys Chem Solids 61:1153–1158
18. Allaouia A, Baia S, Chengb HM, Bai JB (2002) Mechanical and electrical properties of a MWNT/epoxy composite. Composite Sci Technol 62:1993–1998
19. Hayashida T, Pan L, Nakayama Y (2002) Mechanical and electrical properties of carbon tubule nanocoils. Physica B 323:352–353
20. Frogley MD, Ravich D, Wagner HD (2003) Mechanical properties of carbon nanoparticle-reinforced elastomers. Composites Sci Technol 63:1647–1654
21. Jiang X, Bin Y, Matsuo M (2005) Electrical and mechanical properties of polyimide–carbon nanotubes composites fabricated by in situ polymerization. Polymer 46:7418–7424
22. Xiaoqing Gao, Lang Liu, Guo Q, Shi J, Zhai G (2005) Fabrication and mechanical/conductive properties of multi-walled carbon nanotube (MWNT) reinforced carbon matrix composites. Mater Lett 59:3062–3065
23. Feng Y, Yuan HL, Zhang M (2005) Fabrication and properties of silver-matrix composites reinforced by carbon nanotubes. Mater Characterization 55:211–218
24. McNallya T, Pötschkeb P, Halleyc P, Murphyc M, Martinc D, Belld SEJ, Brennane GP, Beinf D, Lemoineg P, Quinn PJ (2005) Polyethylene multiwalled carbon nanotube composites. Polymer 46:8222–8232
25. Yamamoto G, Sato Y, Takahashi T, Omori M, Okubo A, Tohji K, Hashida T (2006) Mechanical properties of binder-free single-walled carbon nanotube solids. Scripta Mater 54:299–303
26. Yakobson BI, Brabec CJ, Bernholc J (1996) Nanomechanics of Carbon Tubes: Instabilities beyond Linear Response. Phys Rev Lett 76:2511–2514
27. Cornwell CF, Wille LT (1997) Elastic properties of single-walled carbon nanotubes in compression. Solid State Commun 101:549–642

28. Hernández E, Goze C, Bernier P, Rubio A (1998) Elastic properties of C and $B_xC_yN_z$ composite nanotubes. Phys Rev Lett 80:4502–4505
29. Sánchez-Portal D, Artacho E, Soler JM, Rubio A, Ordejón P (1999) Ab initio structural, elastic, and vibrational properties of carbon nanotubes. Phys Rev B 59:12678–12688
30. Buongiorno Nardelli M, Fattebert J-L, Orlikowski D, Roland C, Zhao Q, Bernholc J (2000) Mechanical properties, defects and electronic behavior of carbon nanotubes. Carbon 38:1703–1711
31. Froudakis GE (2001) Hydrogen interaction with single-walled carbon nanotubes: a combined quantum-mechanics/molecular-mechanics study. Nano Lett 1:179–182
32. Guo Y, Guo W (2003) Mechanical and electrostatic properties of carbon nanotubes under tensile loading and electric field. J Phys D Appl Phys 36:805–811
33. Williams KA, Eklund PC (2000) Monte Carlo simulations of H_2 physisorption in finite-diameter carbon nanotube ropes. Chem Phys Lett 320:352–358
34. Levesque D, Gicquel A, Darkrim FL, Kayiran SB (2002) Monte Carlo simulations of hydrogen storage in carbon nanotubes. J Phys: Condens Matter 14:9285–9293
35. Hasan S, Guo J, Vaidyanathan M, Alam MA, Lundstrom M (2004) Monte-Carlo simulation of carbon nanotube devices. IEEE-International Workshop on Computational Electronics, October 24–27, 2004, Purdue University, West Lafayette, Indiana, USA
36. Yao N, Lordi V (1998) Young's modulus of single-walled carbon nanotubes. J Appl Phys 84:1939–1943
37. Jin Y, Yuan FG (2003) Simulation of elastic properties of single-walled carbon nanotubes. Composite Sci Technol 63:1507–1515
38. Chang T, Gao H (2003) Size-dependent elastic properties of a single-walled carbon nanotube via a molecular mechanics model. J Mech Phys Solids 51:1059–1074
39. Liew KM, He XQ, Wong CH (2004) On the study of elastic and plastic properties of multi-walled carbon nanotubes under axial tension using molecular dynamics simulation. Acta Mater 52:2521–2527
40. Liew KM, Wong CH, Tan MJ (2006) Tensile and compressive properties of carbon nanotube bundles. Acta Mater 54:225–231
41. Wong EW, Sheehan PE, Lieber CM (1997) Nanobeam mechanics: elasticity, strength, and toughness of nanorods and nanotubes. Science 277:1971–1975
42. Sohlberg K, Sumpter BG, Tuzun RE, Noid DW (1998) Continuum methods of mechanics as a simplified approach to structural engineering of nanostructures. Nanotechnology 9:30–36
43. Govindjee S, Sackman JL (1999) On the use of continuum mechanics to estimate the properties of nanotubes. Solid State Commun 110:227–230
44. Ru CQ (2000) Column buckling of multiwalled carbon nanotubes with interlayer radial displacements. Phys Rev B 62:16962–16967
45. Srivastava D, Menon M, Cho K (2001) Computational nanotechnology with carbon nanotubes and fullerenes. Comput Sci Eng 3:42–55
46. Harik VM (2002) Mechanics of carbon nanotubes: applicability of the continuum-beam models. Comput Mater Sci 24:328–342
47. Liu YJ, Chen XL (2003) Continuum models of carbon nanotube-based composites by the BEM. Electr J Boundary Elem 1:316–335
48. Liu YJ, Chen XL (2003) Evaluations of the effective materials properties of carbon nanotube-based composites using a nanoscale representative volume element. Mech Mater 35:69–81
49. Chen XL, Liu YJ (2004) Square representative volume elements for evaluating the effective material properties of carbon nanotube-based composites. Comput Mater Sci 29:1–11
50. Xiao T, Liao K (2004) A nonlinear pullout model for unidirectional carbon nanotube-reinforced composites. Composite Part B 35:211–217
51. Wang XY, Wang X (2004) Numerical simulation for bending modulus of carbon nanotubes and some explanations for experiment. Composite Part B 35:79–86
52. Liu Y, Nishimura N, Otani Y (2005) Large-scale modeling of carbon-nanotube composites by fast multipole boundary element method. Comput Mater Sci 34:173–187
53. Kireitseu M, Kompis V, Altenbach H, Bochkareva V, Hui D, Eremeev S (2005) Continuum mechanics approach and computational modelling of submicrocrystalline and nanoscale materials. Fullerenes Nanotubes Carbon Nanostruct 13:313–329
54. Tserpesa KI, Papanikos P (2005) Finite element modeling of single-walled carbon nanotubes. Composite Part B 36:468–477
55. Ashrafi B, Hubert P (2006) Modeling the elastic properties of carbon nanotube array/polymer composites. Composite Sci Technol 66:387–396
56. Hone J, Whitney M, Piskoti C, Zettl A (1999) Thermal conductivity of single walled nanotubes. Phys Rev B 59:2514–2516
57. Yi W, Lu L, Dian-lin Z, Pan ZW, Xie SS (1999) Linear specific heat of carbon nanotubes. Physical Review B 59, pp. 9015–9018
58. Kim P, Shi L, Majumdar A, McEuen PL (2001) Thermal transport measurement of individual multiwalled nanotubes. Phys Rev Lett 87:215502 (1–4)
59. Berber S, Kwon YK, Tomanek D (2000) Unsually high thermal conductivity of carbon nanotubes. Phys Rev Lett 84:4613–4616
60. Osman MA, Srivastava D (2001) Temperature dependence of the thermal conductivity of single walled carbon nanotube Nanotechnol 12:21–24
61. Che J, Cagin T, Goddard III WA (2001) Thermal conductivity of carbon nanotubes. Nanotechnology 11:65–69
62. Biercuk MJ, Llaguno MC, Radosavljevic M, Hyun JK, Johnson AT, Fischer JE (2002) Carbon nanotube composites for thermal management. Appl Phys Lett 80:2767–2769
63. Maruyama S (2003) A molecular dynamics simulation of heat conduction of a finite length single-walled carbon nanotube. Microscale Thermophys Eng 7:41–50
64. Moreland JF, Freund JB, Chen G (2004) The disparate thermal conductivity of carbon nanotubes and diamond nanowires studied by atomistic simulation. Microscale Thermophys Eng 8:61–69
65. Xu Y, Ray G, Abdel-Magid B (2006) Thermal behavior of single-walled carbon nanotube polymer-matrix composites. Composite Part A (in press)
66. Nishimura N, Liu YJ (2004) Thermal analysis of carbon-nanotube composites using a rigid-line inclusion model by the boundary integral equation method. Comput Mech 35:1–10
67. Zhang J, Masa. Tanaka, Matsumoto T, Guzik A (2004) Heat conduction analysis in bodies containing thin walled structures by means of hybrid BNM with an application to CNT-based composites. JSME Int J 47:181–188
68. Zhang J, Masa. Tanaka, Matsumoto T (2004) A simplified approach for heat conduction analysis of CNT-based nano composites. Comput Meth Appl Mech Eng 193:5597–5609
69. Masa. Tanaka, Zhang J, Matsumoto T (2003) Multi-domain hybrid BNM for predicting thermal properties of CNT composites. Asia-Pacific International Conference on Computational Methods in Engineering 5–7 November, Sapporo, Japan, pp 3–12
70. Singh IV, Sandeep K, Prakash R (2004) Application of meshless element free Galerkin method in two-dimensional heat conduction problems. Comput Assist Mech Eng Sci 11:265–274
71. Singh IV (2004) Meshless EFG method in 3-D heat transfer problems: a numerical comparison, cost and error analysis. Numer Heat Transfer Part A 46:192–220
72. Singh IV (2005) A numerical study of weight functions, scaling and penalty parameters for heat transfer applications. Numer Heat Transfer Part A 47:1025–1053